

# Thermodynamics of protein folding and molecular recognition

Ernesto Freire

Department of Biology and Biocalorimetry Center,  
The Johns Hopkins University, Baltimore, MD 21218

*Abstract:* The successful development of a structural parameterization of the energetics of protein folding has permitted the incorporation of the functions that define the enthalpy, entropy and heat capacity changes (i.e. the individual components of the Gibbs energy) into a statistical thermodynamic formalism that describes the equilibrium folding pathway of a protein. The general approach is to construct with the computer a large ensemble of conformational states, and then derive the most probable population distribution; i.e. the distribution of states that best accounts for a wide array of experimental observables. The accuracy of the approach is evaluated by comparison of predicted and experimental physical observables. This formalism has allowed the development of a computer program (Virtual Differential Scanning Calorimetry, VDSC) that generates the expected heat capacity function from a PDB data file containing the atomic coordinates of a protein; and a second program (CoreFHT) that predicts the NMR derived hydrogen exchange protection factors for individual amino acids.

## INTRODUCTION

The prediction of the folding energetics of proteins from structural considerations has been a major challenge for over three decades. In particular, attempts at using small molecule models have been unable to account quantitatively for the folding energetics. In 1969, Lumry and Biltonen (1) stated that “*at present it appears improbable that small molecules can serve as more than a rough guide toward a description of the quantitative aspects of protein folding. It is undoubtedly true that studies of small-molecule models can improve our qualitative understanding of protein construction, but the use of these models in a quantitative way is so complex and involves so many parameters that we must for many years mistrust inevitable claims that specific aspects of structure are “explained” by the very rough theories now possible*”. Twenty seven years later those words are still true and not because of a lack of effort from a significant number of scientists. It has become clear that the energetics of protein folding cannot be rationalized by adding up the contributions measured for individual groups in small model compounds. While some interactions appear to obey group additivity (e.g. the energetics of hydration of apolar groups or the heat capacity changes) others do not, notably the energetics of hydration of polar groups or internal interactions (2-4). Certainly, the solution to the problem requires a different approach.

Currently, the most successful attempts at parameterizing the folding energetics in terms of structure incorporate a statistical analysis of protein data combined with a rigorous statistical mechanical evaluation of those functions that cannot be measured experimentally (e.g. conformational entropy) (4-9). The statistical analysis is aimed at establishing precise correlations between energetic parameters measured directly on proteins and highly resolved structural features of the protein. This approach has demonstrated to be highly accurate and to have the predictive potential necessary for its utilization in molecular design strategies. The goal of this approach is the prediction of the Gibbs energy and consequently the probability of an arbitrary conformation of a protein. Very recently, CALVIN, the first algorithm for energy minimization of protein conformations using the structural parameterization of the energetics has been developed (Luque and Freire, in preparation). This algorithm is currently being employed in the design of protease inhibitors.

More than thirty years ago, the two-state model became a paradigm for the interpretation of protein folding/unfolding data (10,11). In more recent years folding/unfolding transitions for multidomain proteins or single domain proteins under conditions in which partially folded states become populated required extensions to this model in order to include several discrete states in the analysis (12-17). In general, the folding/unfolding equilibrium of proteins as observed by global macroscopic observables can be usually described by those models. The situation is different, however, when the equilibrium is studied by physical observables that monitor the behavior of individual residues, like NMR detected hydrogen

exchange protection factors. It is clear that simple two-state, three-state or other models that only include a few discrete states cannot account for these observables even under conditions in which folding/unfolding transitions are well accounted for by these models. (18-30). The interpretation and analysis of this type of data requires a statistical ensemble of conformational states as demonstrated recently (31,32).

In the past, statistical thermodynamic models of protein folding have been based upon extremely oversimplified pictures of proteins and therefore have lacked the capability for data analysis. Statistical thermodynamic models have usually been aimed at capturing general, yet coarse features of proteins rather than quantitative prediction. The development of an accurate structural parameterization of the energetics has opened the doors to a direct statistical thermodynamic interpretation and analysis of experimental data. The strategy is conceptually simple: 1) use the high resolution structure of a protein as a template to derive a large ensemble of partially folded conformations; 2) calculate the Gibbs energy of each conformation; 3) evaluate the probability distribution of states; and, 4) predict experimental observables. Two computer programs (VDSC and CoreFHT) that implement this formalism have been created and will be discussed in this presentation.

## STRUCTURAL PARAMETERIZATION OF FOLDING ENERGETICS

The most important quantity in the thermodynamic description of folding or binding is the Gibbs energy ( $\Delta G$ ) which is completely specified if the enthalpy ( $\Delta H$ ), entropy ( $\Delta S$ ) and heat capacity ( $\Delta C_p$ ) changes are known at some reference temperatures ( $T_R$ ):

$$\Delta G = \Delta H(T) - T \cdot \Delta S(T) \quad (1)$$

$$\Delta H(T) = \Delta H(T_R) + \int_{T_R}^T \Delta C_p \, dT \quad (2)$$

$$\Delta S(T) = \Delta S(T_R) + \int_{T_R}^T \Delta C_p \, d \ln T \quad (3)$$

In most cases, the contributions to the Gibbs energy of folding or binding can be separated into the following main terms:

$$\Delta G = \Delta G_{\text{gen}} + \Delta G_{\text{ion}} + \Delta G_{\text{tr}} \quad (4)$$

where  $\Delta G_{\text{gen}}$  contains the contributions typically associated with the formation of secondary and tertiary structure (van der Waals interactions, hydrogen bonding, hydration and conformational entropy),  $\Delta G_{\text{ion}}$  the ionization effects, and  $\Delta G_{\text{tr}}$  the contribution of the change in translational degrees of freedom in the case of binding or folding coupled to oligomerization (33). According to equations 2 and 3, the enthalpy and entropy changes need to be evaluated at some reference temperature and then extrapolated to the desired temperature by using the heat capacity change. The choice of reference temperatures for enthalpy and entropy changes is a matter of convenience and usually represent temperatures at which experimental data are more easily acquired or temperatures at which some property exhibits a special behavior. So for example, for enthalpy changes the reference temperature has been chosen as 60°C which corresponds to the median denaturation temperature of proteins and represents a temperature at which the experimental values contain the lowest error. For entropy changes, on the other hand, the reference temperatures correspond to temperatures at which hydration entropies are zero.

### The Structural/Solvation Contributions to the Gibbs Energy

The structural contributions are contained in the term  $\Delta G_{\text{gen}} = \Delta H_{\text{gen}} - T \cdot \Delta S_{\text{gen}}$  which is calculated by estimating separately the enthalpy and entropy contributions. The important structural changes for these calculations are the changes in apolar and polar solvent accessible surface areas ( $\Delta \text{ASA}_{\text{ap}}$  and  $\Delta \text{ASA}_{\text{pol}}$ ) and the distribution of interatomic distances between different atom types which determines the packing density. The changes in accessible surface areas are calculated using the Lee and Richards algorithm (34) using a solvent radius of 1.4Å and a slice width of 0.25Å. When the solvent accessibilities of the unfolded conformations are needed, a set of free energy optimized values is used (9).

*a) The Enthalpy Change.* The bulk of the enthalpy change scales in terms of  $\Delta\text{ASA}$  changes and packing density and at the reference temperature of 60°C it can be written as

$$\Delta H_{\text{gen}}(60) = (\alpha_{\text{ap}} + \beta_{\text{ap}} \cdot U_{\text{ap}}^6) \cdot \Delta\text{ASA}_{\text{ap}} + (\alpha_{\text{pol}} + \beta_{\text{pol}} \cdot U_{\text{pol}}^6) \cdot \Delta\text{ASA}_{\text{pol}} + \beta_{\text{mix}} \cdot U_{\text{mix}}^6 \cdot \Delta\text{ASA}_{\text{Total}} \quad (5)$$

where the empirical coefficients  $\alpha$  and  $\beta$  have been estimated from an analysis of the protein thermodynamic database and are equal to  $\alpha_{\text{ap}} = -12.96$ ,  $\beta_{\text{ap}} = 25.34$ ,  $\alpha_{\text{pol}} = 24.38$ ,  $\beta_{\text{pol}} = 16.57$  and  $\beta_{\text{mix}} = 16.42$ . The terms  $U_i$  represent the packing density of apolar, polar and mixed atoms and is equal to the energy weighted average of the ratio between the separation distance at the minimum in the potential well and the actual separation between atom types. For the average packing density observed at protein interiors, equation 5 reduces to

$$\Delta H_{\text{gen}}(60) = -8.44 \cdot \Delta\text{ASA}_{\text{ap}} + 31.4 \cdot \Delta\text{ASA}_{\text{pol}} \quad (6)$$

At any other temperature,  $\Delta H_{\text{gen}}(T)$  is obtained from the standard thermodynamic equation:

$$\Delta H_{\text{gen}}(T) = \Delta H_{\text{gen}}(60) + \Delta C_p \cdot (T - 333.15) \quad (7)$$

*b) The Entropy Change.* In the calculation of the entropy change two primary contributions are included, one due to changes in solvation and the other due to changes in conformational degrees of freedom ( $\Delta S_{\text{gen}}(T) = \Delta S_{\text{solv}}(T) + \Delta S_{\text{conf}}$ ). The entropy of solvation is temperature dependent while the conformational entropy is essentially a constant at different temperatures. The entropy of solvation can be written in terms of the heat capacity if the temperatures at which the apolar and polar hydration entropies are zero ( $T_{\text{S,ap}}^*$  and  $T_{\text{S,pol}}^*$ ) are used as reference temperatures:

$$\Delta S_{\text{solv}}(T) = \Delta S_{\text{solv,ap}}(T) + \Delta S_{\text{solv,pol}}(T) \quad (8a)$$

$$\Delta S_{\text{solv}}(T) = \Delta C_{p,\text{ap}} \cdot \ln(T/T_{\text{S,ap}}^*) + \Delta C_{p,\text{pol}} \cdot \ln(T/T_{\text{S,pol}}^*) \quad (8b)$$

$T_{\text{S,ap}}^*$  has been known to be equal to 385.15K for some time (35,36) and  $T_{\text{S,pol}}^*$  has been recently found to be close to 335.15K (4). While the entropy of apolar solvation appears to be additive, the situation for polar solvation is known to depend on the number and density of polar functional groups in the molecule (2).

Conformational entropies upon binding or folding are evaluated by explicitly considering the following three contributions for each amino acid: 1)  $\Delta S_{\text{bu} \rightarrow \text{ex}}$ , the entropy change associated with the transfer of a side chain that is buried in the interior of the protein to its surface; 2)  $\Delta S_{\text{ex} \rightarrow \text{u}}$ , the entropy change gained by a surface exposed side chain when the peptide backbone changes from a unique conformation to an unfolded conformation; and, 3)  $\Delta S_{\text{bb}}$ , the entropy change gained by the backbone itself upon unfolding from a unique conformation. The magnitude of these terms for each amino acid has been estimated by computational analysis of the probability of different conformers as a function of the dihedral and torsional angles (4,8,9). Other conformational entropy terms like those arising from conformational restrictions due to the presence of disulfide bridges are estimated as described in the literature (see for example reference (37)).

*c) The Heat Capacity Change.* The heat capacity change is a weak function of temperature and has been parameterized in terms of changes in solvent accessible surface areas ( $\Delta\text{ASA}$ ) since it originates mainly from changes in hydration (5,6,38):

$$\Delta C_p = \Delta C_{p,\text{ap}} + \Delta C_{p,\text{pol}} \quad (9a)$$

$$\Delta C_p = a_C(T) \cdot \Delta\text{ASA}_{\text{ap}} + b_C(T) \cdot \Delta\text{ASA}_{\text{pol}} + c_C(T) \cdot \Delta\text{ASA}_{\text{OH}} \quad (9b)$$

where the coefficients  $a_C(T) = 0.45 + 2.63 \times 10^{-4} \cdot (T - 25) - 4.2 \times 10^{-5} \cdot (T - 25)^2$  and  $b_C(T) = -0.26 + 2.85 \times 10^{-4} \cdot (T - 25) + 4.31 \times 10^{-5} \cdot (T - 25)^2$ . The hydration of the hydroxyl group in aliphatic hydroxyl side chains (Ser and Thr) appears to contribute positively and not negatively to  $\Delta C_p$  as previously assumed (0.17 cal/K·mol Å<sup>2</sup> at 25°C) (38). In the equation above,  $\Delta\text{ASA}$  changes are in Å<sup>2</sup> and the heat capacity in cal/K·mol. In general, for low temperature calculations ( $T < 80^\circ\text{C}$ ) the temperature independent coefficients are sufficient (6,38). Specific effects like heat capacity changes associated to changes in protonation, differential binding of ligands or denaturants, etc. need to be considered individually (6,38).

### The Contributions of Ionization to the Gibbs Energy

In most cases, the folding/unfolding equilibrium is coupled to the protonation/deprotonation of one or more groups in the protein. If this is the case, the protonation contribution to the Gibbs energy of an arbitrary conformational state  $j$  is equal to :

$$\Delta G_{\text{ion},j} = -R \cdot T \cdot \text{Ln} \left( \prod_i \frac{(1 + 10^{pK_{j,i} - \text{pH}})}{(1 + 10^{pK_{N,i} - \text{pH}})} \right) \quad (10)$$

where  $pK_{j,i}$  is the  $pK$  of group  $i$  in state  $j$  and  $pK_{N,i}$ , the  $pK$  of group  $i$  in the reference state which in this case is the native state. According to equation 10, at any  $\text{pH}$  the additional contribution of protonation to  $\Delta G$  can be calculated if the  $pK$  of that group is known in the protein conformations under consideration. Traditionally, the  $pK$  of different groups in proteins have been estimated experimentally. Recently, however, serious attempts have been made at predicting  $pK$ 's from structure (39). It is expected that within the next few years, protonation effects will be accurately parameterized in terms of structure and that accurate prediction of protein stability as a function of  $\text{pH}$  will be possible.

## THE STATISTICAL NATURE OF PROTEIN FOLDING

Proteins cannot be considered as an equilibrium between two or a few discrete conformational states since the number of conformations that are available to them is astronomically large. Under equilibrium conditions, the population of protein conformations in solution is dictated by the Gibbs energy of each state. Depending on the exact experimental conditions (native, denaturing, transition, etc.) the native, unfolded or some other conformation will predominate. The probability of any given conformational state,  $P_i$ , is given by the equation:

$$P_i = \frac{\exp(-\Delta G_i / RT)}{Q} \quad (11)$$

where the statistical weights or Boltzmann exponents ( $\exp(-\Delta G_i / RT)$ ) are defined in terms of the relative Gibbs energies  $\Delta G_i$  for each state ( $R$  is the gas constant and  $T$  the absolute temperature).  $Q$  is the conformational partition function defined as the sum of the statistical weights of all the states accessible to the protein:

$$Q = \sum_{i=0}^N \exp(-\Delta G_i / RT) \quad (12)$$

The relative Gibbs energy of each state ( $\Delta G_i$ ) is expressed in terms of the standard thermodynamic equation:

$$\Delta G_i = \Delta H_i - T \cdot \Delta S_i \quad (13)$$

where  $\Delta G_i$ ,  $\Delta H_i$  and  $\Delta S_i$  are the relative Gibbs energy, enthalpy and entropy of state  $i$  at temperature  $T$ , respectively.

In the past, the statistical thermodynamic analysis of the experimentally observed folding/unfolding equilibrium has been extremely difficult if not impossible. The situation has changed with the development of NMR detected hydrogen exchange and its unique ability to monitor simultaneously the behavior of a large number of residues (18-30).

The interpretation or analysis of hydrogen exchange protection factors or other residue-level observables requires the introduction of a new type of statistical descriptor: the apparent stability constant per residue (31,32). The apparent stability constant per residue,  $K_{f,j}$ , is defined as the ratio of the probabilities of all states in which residue  $j$  is folded,  $P_{f,j}$ , to the probabilities of the states in which residue  $j$  is not folded:

$$\kappa_j = \frac{\sum_{\substack{\text{(states with} \\ \text{residue j folded)}} P_i}{\sum_{\substack{\text{(states with} \\ \text{residue j not folded)}} P_i} = \frac{P_{f,j}}{P_{nf,j}} \quad (14)$$

The apparent folding constant per residue,  $\kappa_{f,j}$ , is the quantity that one will measure if it were possible to experimentally determine the stability of the protein by monitoring each individual residue. The corresponding apparent free energy per residue is simply  $\Delta G_{f,j} = -R \cdot T \cdot \ln \kappa_{f,j}$ . In many cases, hydrogen exchange protection factors are equal to the apparent folding constants per residue. In general, however, hydrogen exchange protection factors are calculated using a modified form of equation 14 as described in references (31,32). The modification accounts for the fact that not all residues that are in the folded state exhibit protection and that some folded residues become exposed because adjacent protein regions (complementary areas) become unfolded.

Global observables, like thermal or chemical denaturation curves, or the heat capacity function measured by differential scanning calorimetry are calculated using standard statistical thermodynamics. The denaturation curve as a function of denaturant concentration can be defined in terms of the average degree of unfolding ( $\langle F_u \rangle$ ) at any denaturant concentration:

$$\langle F_u \rangle = \sum F_{u,i} \cdot P_i \quad (15)$$

where  $F_{u,i}$  is the fractional degree of unfolding of state  $i$  (i.e. the number of unfolded residues in state  $i$  divided by the total number of residues) and  $P_i$  the probability of state  $i$  given by equation 11. The excess heat capacity function,  $\langle \Delta C_p \rangle$ , is defined as

$$\langle \Delta C_p \rangle = \sum (\Delta H_i \cdot (\partial P_i / \partial T) + P_i \cdot \Delta C_{p,i}) \quad (16)$$

where the summation runs over all states in the ensemble.

## THE COREX ALGORITHM.

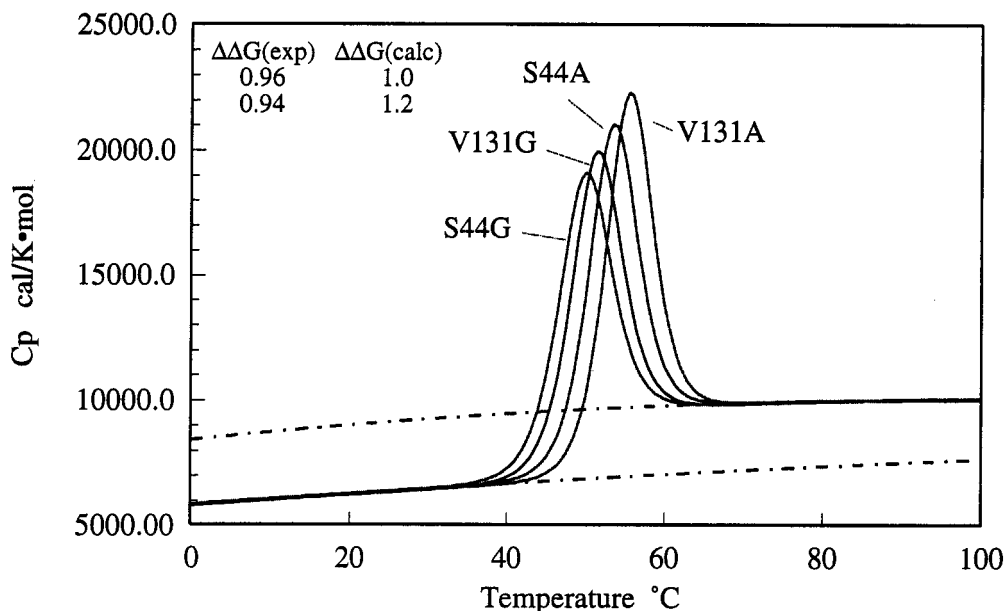
Analysis of protein equilibrium in terms of the formalism described above involves an approximation of the ensemble of conformational states available to a protein. In our laboratory, the ensemble of partially folded states is approximated with the computer by using the high resolution structure as a template. In the COREX algorithm (31,32) the entire protein is considered as being composed of different folding units and partially folded states are generated by folding and unfolding those units in all possible combinations.

The division of the protein into a given number of folding units is called a partition. In order to maximize the number of distinct partially folded states, different partitions are included in the analysis. Each partition is defined by placing a block of windows over the entire sequence of the protein. The folding units are defined by the location of the windows irrespective of whether or not they coincide with specific secondary structure elements. By sliding the entire block of windows one residue at a time different partitions of the protein are obtained. For two consecutive partitions the first and last amino acids of each folding unit are shifted by one residue. This procedure is repeated until the entire set of partitions have been exhausted. Usually, 50,000 - 150,000 states are generated for a typical globular protein.

Each of the states generated by the COREX algorithm is characterized by having some regions folded and some other regions unfolded. There are two basic assumptions in this algorithm: 1) The folded regions in partially folded states are native-like; and, 2) the unfolded regions are assumed to be devoid of structure. While these assumptions appear drastic at first, it has been shown that the resulting ensemble accounts well for the global stability and cooperativity of proteins as well as hydrogen exchange protection patterns. These observations suggest that those states not included in the ensemble (e.g. non native-like intermediates) have vanishingly small probabilities and do not contribute measurably to the experimental values under normal equilibrium conditions.

## VIRTUAL DIFFERENTIAL SCANNING CALORIMETRY (VDSC)

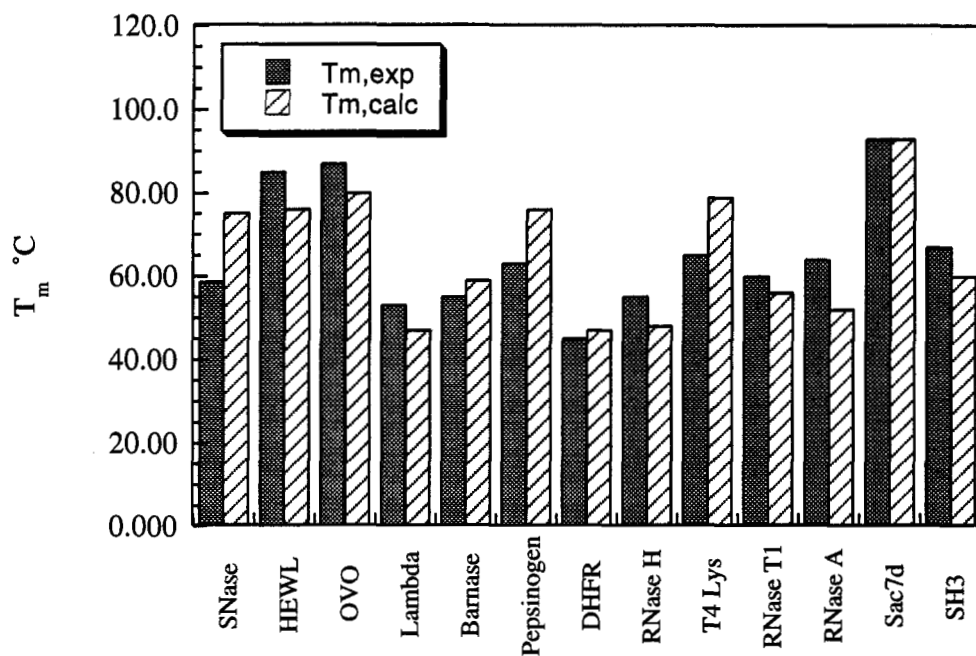
Figure 1 shows the heat capacity function generated by VDSC for four different single amino acid mutants of T4 lysozyme at pH 3.2. Under these conditions, the experimental transition temperature is 52.9°C for the S44A mutant compared to the calculated value of 53.6°C. Replacement of the alanine at position 44 by glycine (S44G) lowers the  $T_m$  by about 3.5°C which is close to the observed experimental change of 2.8. Rather similar results are obtained for the mutations at position 131. The difference between  $\Delta\Delta G$  values are also very close as indicated in the figure. These results underscore the ability of VDSC to predict the effect of amino acid mutations on the stability of a protein and therefore its utility in protein design.



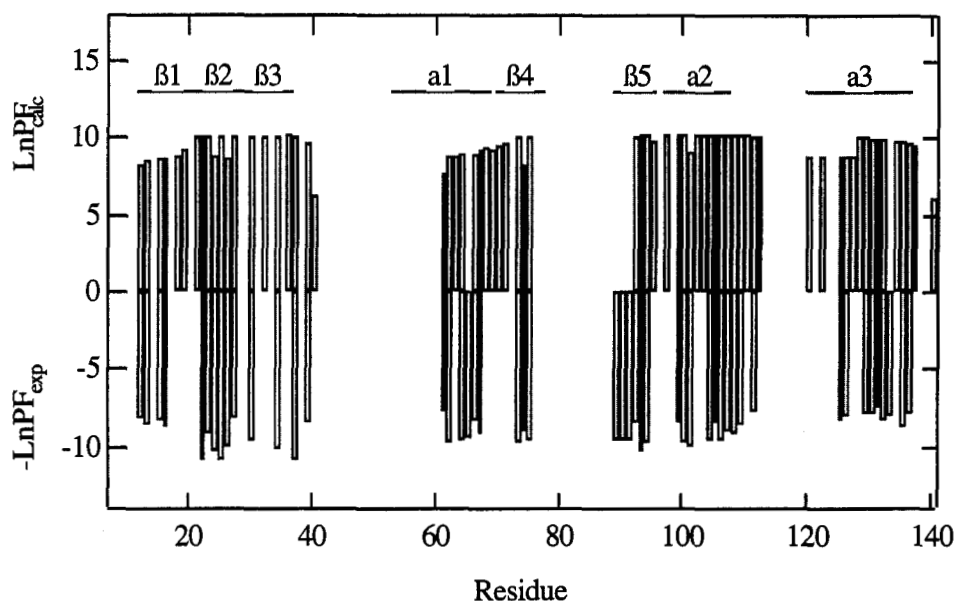
**Fig. 1.** The heat capacity function versus temperature for four mutants of T4 lysozyme under conditions in which the folding/unfolding obeys two-state behavior. Shown as dotted lines are the heat capacities of the native and unfolded states. The curves were generated by the computer program VDSC v1.0. VDSC directly reads a PDB file and generates the structure-based thermodynamic analysis. The simulated conditions in the figure correspond to pH 3.2. For these calculations, the structures of the mutants were derived from that of the pseudo wild type C54T/C97A structure which is the template used for the experimental Ala and Gly mutations. These mutations are at solvent exposed locations and have been shown to have essentially superimposable structures (40). Figure adapted from reference (41).

Figure 2 summarizes the predicted and experimental transition temperatures for thirteen different proteins. In this case, VDSC performed the analysis at the indicated pH which corresponds to the pH range at which the stability of the protein is maximal. The mean value of the difference between predicted and experimental  $T_m$  values is  $-0.2$  with a standard deviation of  $\pm 9.5$  °C.

It has been shown, that the structural parameterization is able to account for the intrinsic helix propensities of each amino acid (9). Application of the analysis to four different systems: T4 lysozyme (54), Barnase (55), a synthetic leucine zipper (56), and a synthetic peptide (57) gave excellent results. For T4 lysozyme, the average value of the absolute difference between predicted and experimental  $\Delta G$  values was 0.09 kcal/mol, for barnase 0.14 kcal/mol, for the synthetic coiled coil 0.11 kcal/mol and for the synthetic peptide 0.08 kcal/mol. Furthermore, for nineteen amino acids a correlation analysis between the results obtained with the structural parameterization and the empirical helix propensity scale developed by Muñoz and Serrano (58) yielded a slope of  $1.089 \pm 0.09$  and a correlation coefficient of 0.94.



**Fig. 2.** Comparison between predicted and experimental  $T_m$  values for thirteen proteins at their pH of maximal stability. Staphylococcal nuclease, pH 7 (16,42); hen egg white lysozyme, pH 5 (43); turkey ovomucoid third domain, pH 5 (44); lambda repressor, pH 7 (Oas, T., personal communication); barnase, pH 6 (45,46); pepsinogen, pH 6 (47); cysteine free dihydrofolate reductase, pH 7 (Pucciarelli, S., unpublished data from this laboratory); cysteine free ribonuclease H, pH 8 (48); T4 lysozyme, pH 5 (49); ribonuclease T1, pH 5 (50); ribonuclease A, pH 6 (51); Sac7d, pH 6 (52); SH3 domain, pH 5 (53). Figure adapted from reference (41).



**Fig. 3.** Comparison of predicted and experimental (22) protection factors at 37°C. For better comparison, the negative value of the experimental protection factors have been plotted in the figure. Shown at the top of both panels are the corresponding elements of secondary structure. Figure adapted from reference (31).

## HYDROGEN EXCHANGE PROTECTION

Figure 3 shows the predicted and experimental (22) hydrogen exchange protection factors for Staphylococcal Nuclease (SNase). The predicted values were obtained as described in references (31,32) using the program CoreFHT.

Inspection of the figure reveals three regions of the protein with major levels of protection. The highest  $\ln PF_i$  values correspond to the second and third  $\beta$  strands (residues 21–39), the central residues of the fourth  $\beta$  strand (residues 73-75) and the last portion of the fifth  $\beta$  strand through the second  $\alpha$  helix (residues 91-106). In this region it must be noted the presence of higher values for the highly hydrophobic cluster Leu36, Leu37, Leu38 and Val39 in  $\beta_3$  and Ala102, Leu103 and Val104 in  $\alpha_2$ . The second level corresponds to the first  $\beta$  strand and the adjacent turns (residues 10-20), the second half of the first  $\alpha$  helix (residues 62-68) along with the beginning of the fourth  $\beta$  strand (residues 71-73), and the region from the loop following the second  $\alpha$  helix through the third helix (residues 107-135). The third level corresponds to the amino and carboxyl terminal residues (7-10 and 136-141) and the loop region from residue 41 to 53, the first half of the first  $\alpha$  helix (residues 54-61) and the loop region defined by residues 77-89.

Of the 49 protected residues, 44 are correctly predicted to exhibit protection. In addition 62 are correctly predicted to show no protection: 6 are prolines, 26 are solvent accessible, and 30 (residues 9, 10, 35, 41, 44-46, 49, 50, 52, 54, 55, 57-60, 77-80, 83, 85-88, 118, 119, 121, 138, and 139) are predicted to have protection factors below the experimental limit of detection. This relatively large number of residues beyond experimental detection is primarily due to the high temperature (37°C) at which the experiments were performed (22). This gives a total of 100 residues (excluding prolines) or 78% for which the prediction matches the experimental results. Of the 29 mispredictions, the vast majority (24) represent cases in which protection was predicted but not observed. This pattern suggests that many of those residues may indeed be thermodynamically stable but able to exchange by a different mechanism. For those residues that exhibit protection, the average difference between predicted and experimental protection factors expressed as differences in the apparent free energies per residue amounts to  $0.3 \pm 0.6$  kcal/mol.

The calculated pattern of protection for SNase involved 163,822 different states, a number large enough to capture the statistical nature of the conformational equilibrium and quantitatively account for the pattern of hydrogen exchange protection.

## CONCLUSIONS

The combination of the structural parameterization of the energetics with a statistical thermodynamic model of the folding equilibrium provides a powerful framework for the analysis of protein folding. It has been shown that accurate prediction of protein stability is possible, and that examination of the most probable distribution of states in the protein ensemble is also possible by analyzing physical observables, like hydrogen exchange protection factors, that report on the state of individual residues. Applications of this approach to molecular design are being developed and will be presented soon.

## ACKNOWLEDGMENT

This work was supported by grants from the National Institutes of Health (RR04328 and GM51362).

## REFERENCES

1. Lumry, R., and Biltonen, R. (1969) in *Biological Macromolecules: Structure and Stability of Biological Macromolecules* (Fasman, S. T. a. G., ed) Vol. II, Marcel Dekker, New York
2. Cabani, S., Gianni, P., Mollica, V., and Lepori, L. (1981) *J. Solution Chem.* **10**(8), 563-595
3. Lazaridis, T., Archontis, G., and Karplus, M. (1995) *Adv. Prot. Chem.* **47**, 231-306
4. DAquino, J. A., Gómez, J., Hilser, V. J., Lee, K. H., Amzel, L. M., and Freire, E. (1996) *Proteins* **25**, 143-156
5. Murphy, K. P., Bhakuni, V., Xie, D., and Freire, E. (1992) *J. Mol. Biol.* **227**, 293-306
6. Gomez, J., Hilser, J. V., Xie, D., and Freire, E. (1995) *Proteins: Structure, Function and Genetics* **22**, 404-412
7. Hilser, V. J., Gomez, J., and Freire, E. (1996) *Proteins In Press*
8. Lee, K. H., Xie, D., Freire, E., and Amzel, L. M. (1994) *Proteins. Struct. Func. and Genetics* **20**, 68-84
9. Luque, I., Mayorga, O., and Freire, E. (1996) *Biochemistry In Press*
10. Lumry, R., Biltonen, R., and Brandts, J. F. (1966) *Biopolymers* **4**, 917-944
11. Privalov, P. L., and Khechinashvili, N. N. (1974) *J. Mol. Biol.* **86**, 665-684
12. Kuwajima, K., Nitta, K., Yoneyama, M., and Sugai, S. (1976) *J. Mol. Biol.* **106**, 359-373



13. Freire, E., and Biltonen, R. L. (1978) *Biopolymers* **17**, 463-479
14. Privalov, P. L. (1982) *Adv. Protein Chem.* **35**, 1-104
15. Montgomery, D., Jordan, R., McMacken, R., and Freire, E. (1993) *Journal of Molecular Biology* **232**, 680-692
16. Xie, D., Fox, R., and Freire, E. (1994) *Protein Science* **3**, 2175-2184
17. Freire, E. (1995) *Ann. Rev. of Biophys. and Biomolec. Struct.* **24**, 141-165
18. Udgaonkar, J. B., and Baldwin, R. L. (1988) *Nature* **335**, 694-699
19. Roder, H., Elove, G. A., and Englander, S. W. (1988) *Nature* **335**, 700-704
20. Radford, S. E., Dobson, C. M., and Evans, P. A. (1992) *Nature* **358**, 302-307
21. Radford, S. E., Buck, M., Topping, K. D., Dobson, C. M., and Evans, P. A. (1992) *Proteins* **14**, 237-248
22. Loh, S. N., Prehoda, K. E., Wang, J., and Markley, J. L. (1993) *Biochemistry* **32**, 11022-11028
23. Kim, K.-S., Fuchs, J. A., and Woodward, C. K. (1993) *Biochemistry* (32), 9600-9608
24. Kim, K.-S., and Woodward, C. (1993) *Biochemistry* **32**, 9609-9613
25. Jennings, P. A., and Wright, P. E. (1993) *Science* **262**, 892-896
26. Jacobs, M. D., and Fox, R. O. (1994) *Proc. Natl. Acad. Sci. USA* **91**, 449-453
27. Woodward, C. (1993) *TIBS* **18**, 359-360
28. Bai, Y., Sosnick, T. R., Mayne, L., and Englander, S. W. (1995) *Science* **269**, 192-197
29. Morozova, L. A., Haynie, D. T., Arico-Muendel, C., Van Dael, H., and Dobson, C. M. (1995) *Nature Structural Biology* **2**, 871-875
30. Schulman, B. A., Redfield, C., Peng, Z., Dobson, C. M., and Kim, P. S. (1995) *J. Mol. Biol.* **253**, 651-657
31. Hilser, V. J., and Freire, E. (1996) *J. Mol. Biol* **In Press**
32. Hilser, V. J., and Freire, E. (1996) *Proteins* **In Press**
33. Murphy, K. P., Xie, D., Thompson, K., Amzel, L. M., and Freire, E. (1994) *Proteins: Struct. Func. Genetics.* **18**, 63-67
34. Lee, B., and Richards, F. M. (1971) *J. Mol. Biol.* **55**, 379-400
35. Baldwin, R. L. (1986) *Proc. Natl. Acad. Sci., USA* **83**, 8069-8072
36. Murphy, K. P., and Freire, E. (1992) *Adv. Protein Chem.* **43**, 313-361
37. Pace, C. N., Grinsley, G. R., Thomson, J. A., and Barnett, B. J. (1988) *J. Biol. Chem.* **263**, 11820-11825
38. Gomez, J., and Freire, E. (1995) *J. Mol. Biol.* **252**, 337-350
39. García-Moreno, B. E. (1995) *Methods Enzymol.* **259**, 512-538
40. Blaber, M., Zhang, X.-j., Lindstrom, J. L., Pepiot, S. D., Baase, W. A., and Matthews, B. W. (1994) *J. Mol. Biol.* **235**, 600-624
41. Hilser, V. J., and Freire, E. (1996) *Biophysical Chem.*
42. Carra, J. H., Anderson, E. A., and Privalov, P. L. (1994) *Protein Science* **3**, 944-951
43. Pfeil, W., and Privalov, P. L. (1976) *Biophys. Chem.* **4**, 23-32
44. Swint-Kruse, L., and Robertson, A. D. (1996) *Biochemistry* **35**, 171-180
45. Martinez, J. C., Harrous, M. E., Filimonov, V. V., Mateo, P. L., and Fersht, A. R. (1994) *Biochemistry* **33**, 3919-3926
46. Griko, Y., Makhatadze, G. I., Privalov, P. L., and Hartley, R. W. (1994) *Protein Science* **3**, 669-676
47. Mateo, P. L., and Privalov, P. L. (1981) *FEBS Lett.* **123**, 189-192
48. Dabora, J. M., and Marqusee, S. (1994) *Protein Science* **3**, 1401-1408
49. Alber, T., Dao-pin, S., Wilson, K., Wozniak, J. A., Cook, S. P., and Matthews, B. W. (1987) *Nature* **330**, 41-46
50. Plaza del Pino, I. M., Pace, C. N., and Freire, E. (1992) *Biochemistry* **31**, 11196-11202
51. Privalov, P. L., Tiktopulo, E. I., and Khechinashvili, N. N. (1973) *Int. J. Pept. Protein Res.* **5**, 229-237
52. McAfee, J. G., Edmondson, S. P., Datta, P. K., Shriver, J. W., and Gupta, R. (1995) *Biochemistry* **34**, 10063-10077
53. Viguera, A. R., Martinez, J. C., Filimonov, V. V., Mateo, P. L., and Serrano, L. (1994) *Biochemistry* **33**, 2142-2150
54. Blaber, M., Zhang, X.-j., and Matthews, B. W. (1993) *Science* **260**, 1637-1640
55. Horovitz, A., Matthews, J. M., and Fersht, A. R. (1992) *J. Mol. Biol.* **227**, 560-568
56. O'Neil, K., and DeGrado, W. (1990) *Science* **250**, 646-651
57. Lyu, P. C., Liff, M. I., Marky, L. A., and Kallenbach, N. R. (1990) *Science* **250**, 669-673
58. Muñoz, V., and Serrano, L. (1995) *J. Mol. Biol.* **245**, 275-296